

**ORIGINAL  
RESEARCH**

M. Zulfiqar  
N. Dumrongpisutikul  
J. Intrapromkul  
D.M. Yousem

# Detection of Intratumoral Calcification in Oligodendrogliomas by Susceptibility-Weighted MR Imaging

**BACKGROUND AND PURPOSE:** SWI is a unique pulse sequence sensitive to both hemorrhage and calcification. Our aim was to retrospectively assess the ability of SWI to detect intratumoral calcification in ODs compared with conventional MR imaging.

**MATERIALS AND METHODS:** Using CT as criterion standard, the MR imaging findings from 71 patients (33 males, 38 females; mean age, 42.5 years) with pathologically proved OD were retrospectively evaluated. We classified the MR imaging data into SWI data (MRSWI) and traditional pulse sequences (MRnoSWI). The sensitivity and specificity of the MRnoSWI ( $n = 71$ ) were compared with that of the MRSWI ( $n = 13$ ) independently and also for matched-paired data ( $n = 13$ ). The Fisher exact test was applied to the matched-pair data for statistical evaluation.

**RESULTS:** For paired data of MRSWI and MRnoSWI ( $n = 13$ ), there was significantly increased sensitivity of MRSWI (86%) for the detection of intratumoral calcification in OD compared with the MRnoSWI (14.3%) ( $P = .015$ , Fisher exact test) by using CT as the criterion standard. The overall accuracy of MRSWI for the paired data was also significantly greater ( $P = .048$ ). The specificities were not significantly different ( $P = .773$ ). The sensitivity of MRSWI ( $n = 13$ ) was 86%, and for MRnoSWI ( $n = 71$ ), it was 33.3%. Specificity of MRSWI was 83%, and for MRnoSWI, it was 95%.

**CONCLUSIONS:** SWI is better able to detect calcification in ODs than conventional MR imaging pulse sequences.

**ABBREVIATIONS:** HP = high-pass; mIP = minimum intensity projection; MRnoSWI = MR without susceptibility-weighted imaging; MRSWI = MR with susceptibility-weighted imaging; OD = oligodendrogloma; SW = susceptibility-weighted; WHO = World Health Organization

SWI is a recently developed pulse sequence used in MR imaging. It makes use of phase images showing local susceptibility changes between tissues that can then be manipulated to measure iron content and other substances that change the local magnetic field. SWI is an excellent tool for the detection of deoxygenated (venous) blood, ferritin, hemosiderin, and deoxyhemoglobin, improving the ability of MR imaging to detect and monitor many neurologic disorders. Stroke, trauma, vascular malformations, vasculopathies, neurodegenerative disorders, and tumors are representative lesions that may benefit from SWI.<sup>1</sup> It has also been proved useful in the applications relating to iron detection, such as measuring the iron content in multiple sclerosis lesions and normal and abnormal aging.<sup>2</sup> More recently, the utility of SWI in the detection of calcification has been explored. The phase images can help differentiate calcification, which is diamagnetic, from hemorrhage, which is paramagnetic.<sup>3,4</sup>

Calcification is a very important factor in the differential diagnosis of brain tumors. Because many tumors have overlapping imaging findings, knowing whether a tumor shows calcification is useful in limiting the differential diagnosis to such lesions that frequently show intratumoral calcification,

such as ODs, craniopharyngiomas, meningiomas, pineal gland tumors, and ependymomas. Among intra-axial brain tumors, ODs have the highest frequency of calcification (approximately 80%).<sup>5,6</sup> Fast spin-echo T1WI, T2WI, and FLAIR MR imaging pulse sequences are considered inferior to CT in detecting and characterizing intracranial calcification.<sup>7,8</sup> Although SWI images have the ability to differentiate hemorrhage from calcification as noted above, this has not been widely studied in the setting of assessing neoplasms for intratumoral calcification. Furthermore, the coexistence of calcification and intratumoral hemorrhage can lead to confusion in assessing neoplasms such as ODs with SWI. The goal of our study was to determine the utility of SWI over conventional pulse sequences for identifying intratumoral calcification in ODs.

## Materials and Methods

The study was approved by the institutional review board as having been compliant with Health Insurance Portability and Accountability Act statutes for expedited review of retrospective imaging studies and did not require patient informed consent.

## Patients

Seventy-one patients with histologic verification of an oligodendroglial tumor (33 males, 38 females; mean age,  $42.5 \pm 14.0$  years; range, 14.5–78.5 years) were enrolled by using query keywords of the radiology information system and pathology database for “oligodendrogloma” during a query period from 2001 to 2010. Demographic data were recorded. CT, MRnoSWI sequences, and MRSWI sequences were independently and retrospectively reviewed and assessed for the

Received May 15, 2011; accepted after revision Aug 2.

From the Russell H. Morgan Department of Radiology and Radiological Science (M.Z., J.I., D.M.Y., N.D.), Johns Hopkins Medical Institutions, Baltimore, Maryland; and King Chulalongkorn Memorial Hospital (N.D.), Pathumwan, Bangkok, Thailand.

Please address correspondence to David M. Yousem, MD, Department of Radiology, Johns Hopkins Medical Institutions, 600 N Wolfe St, Phipps B100F, Baltimore, MD 21287; e-mail: dyousem1@jhu.edu

<http://dx.doi.org/10.3174/ajnr.A2862>

presence or absence of calcification in the tumors by 3 neuroradiologists blinded to the results of the other technique. In this study, we excluded the patients with histopathologic reports outside our hospital.

### Imaging Techniques

**CT.** CT scans were obtained with a soft-tissue and bone algorithm by using a 0.75-mm thickness and reconstructed at 5-mm-thick sections. Further CT parameters were as follows: x-ray tube current = 400 mAs, 120 kVP, and FOV = 23.4 cm.

**MR Imaging.** The MR imaging studies were performed with different MR imaging machines: GE Healthcare (Milwaukee, Wisconsin), Philips Healthcare (Best, the Netherlands), and Siemens (Erlangen, Germany), operating at either 1.5 or 3T. Diffusion-weighted, T1WI, fast spin-echo T2WI, fast spin-echo FLAIR, and postgadolinium T1WI were performed in addition to SWI.

The sagittal T1WI was obtained with parameters as follows: range of TRs, 9.89–696 ms and TEs, 4.6–14 ms; matrix size range from 192 × 192 to 512 × 196; FOV range from 190 × 190 mm to 240 × 240 mm; and range of section thickness/spacing from 1/1 to 5/7 mm.

The axial T2WI was obtained with the range of TR, 2500–7000 ms and TE, 83.136–112 ms; matrix size range from 256 × 184 to 448 × 335; FOV range from 159 × 200 mm to 240 × 240 mm; and the range of section thickness/spacing from 2/2 to 5/5-mm.

FLAIR scan parameters were the following: TR, 6000 ms; TE, 120 ms; TI, 2000 ms; section thickness, 5 mm; FOV, 23 cm; and matrix size, 256 × 256.

**SWI.** The SWI sequences were performed only on the Siemens magnet. The imaging parameters for the SWI sequence were the following: TR/TE, 48/40 ms; flip angle, 15°; phase direction, 0.9 mm; frequency direction, 0.8 mm; section thickness, 1.2 mm; FOV, 200 × 162 mm; matrix size, 256 × 217.

### Image Data Processing

Two radiologists retrospectively reviewed the CT and MR images blinded to the pathologic grade of the OD and the results of the other studies. The location of the calcification on CT was correlated with the MRSWI and MRnoSWI images on the basis of anatomic landmarks so as to adjust for section thicknesses, angulation, and obliquity. Reviews of the image data (CT versus MR imaging) were spaced out during at least 2 weeks in separate sessions by 2 reviewers. In the event of disagreements between reviewers, a third neuroradiologist adjudicated between them with an independent review. The 13 cases that had SWI sequences were read at separate intervals with and without the SWI sequences for the detection of calcification. The Fisher exact test was used to signify a statistical difference between the 2 sequences for the matched-paired data.

### Statistical Analysis

By using CT as the criterion standard, we acquired decision matrix data of 71 MR imaging cases for the detection of calcification in ODs. Seventy-one were MRnoSWI. Of these 71 that were reviewed without SWI sequences included, 13 had additional SWI data (MRSWI) and were subsequently reviewed after a 4-week delay. Independent sensitivity and specificity of the 2 methods of imaging were obtained. Among the 13 subjects with both standard pulse sequences and SWI sequences, matched sample data were obtained and independently reviewed with a 4-week gap between analyses (Table 1). Using these paired data, we performed the Fisher exact test for sensitivity and

**Table 1: Decision matrix data for the detection of calcification in ODs for MRSWI and MRnoSWI<sup>a</sup> versus CT (criterion standard)**

	CT+	CT–
MRSWI +	6	1
–	1	5
MRnoSWI +	1	1
–	6	5

**Note:**—+ indicates test was positive for calcification; –, test was negative for calcification.

<sup>a</sup> *n* = 13, paired. The same cases but read without SWI sequences.

specificity. Microsoft Excel Version 2009 (Bothell, Washington) was used. A *P* value of < .05 was considered statistically significant.

### Results

All 71 subjects in the study had the histopathologic diagnoses of OD. Calcification was present by CT scanning, the criterion standard, in 27 of 71 cases (38%). Among the MR imaging studies of the 71 subjects, 13 had both MRnoSWI and MRSWI sequences and 58 did not have SWI data. Using CT as the criterion standard, MRSWI (*n* = 13) was 85.7% sensitive (6/7) and 83.3% (5/6) specific for intratumoral calcification. MRnoSWI (*n* = 71) was 33.3% (9/27) sensitive and 95.5% specific (42/44) for calcification (Table 2). The Fisher exact test of the 13 sets of paired data yielded a 1-tailed *P* value of .015 for the increased sensitivity of MRSWI (85.7% = 6/7) versus MRnoSWI (14.3% = 1/7) to detect intratumoral calcification in ODs. For specificity, the Fisher exact test yielded a 1-tailed *P* value of .773; hence, there was no statistically significant difference in the specificity between MRnoSWI and MRSWI. The accuracy of MRSWI was also significantly greater than MRnoSWI (*P* = .048).

Of the MRSWI cases, CT showed calcification in 7/13 (Fig 2–4). Of these 7, calcification was detected by MRSWI in 6/7 cases and was negative for calcification in 1/7 cases. Both MRSWI and CT studies showed absence of calcification in 5/13 cases and the assessment for calcification negative on CT but positive on SWI (ie, false-positive) in 1/13 cases.

In MRnoSWI cases, CT showed calcification in 27/71. Of these 27 CT-positive cases, MRnoSWI was positive in 9 cases but negative in 18 cases. Both CT and MR imaging were negative in 42/71 and the assessment for calcification negative by CT but positive by MR imaging in 2/71 (false-positive) cases (Table 3).

In the subset of the MRnoSWI cases that also had SWI data (*n* = 13), the MRnoSWI showed calcification in 1 of the 7 CT-positive cases and no calcification in 6 cases. Both CT and MR imaging were negative for calcification in 5/13 and the assessment for calcification negative by CT but positive by MR imaging in 1/13 (false-positive) cases.

### Discussion

SWI provides a new type of contrast in MR imaging that is complementary to spin attenuation, T1WI, or T2WI. This method exploits the susceptibility differences between tissues and uses a full velocity-compensated radio-frequency-spoiled high-resolution 3D gradient-echo scan.<sup>1</sup>

Even though using SWI to detect calcification is an area of research interest, SWI has the highest utility in the detection of deoxygenated venous blood. The iron in deoxyhemoglobin in venous blood acts as an intrinsic contrast agent, causing shift

**Table 2: Sensitivity, specificity, PPV, NPV, and accuracy of MRSWI versus MRnoSWI for detection of calcification in ODs compared with our criterion standard CT**

	MRSWI (n = 13)	MRnoSWI <sup>a</sup> (n = 13)	P Value <sup>b</sup>	MRnoSWI <sup>c</sup> (n = 71)
Sensitivity (%)	86 (6/7)	14.3 (1/7)	.015	33 (9/27)
Specificity (%)	83 (5/6)	83 (5/6)	NS	95 (42/44)
PPV (%)	86 (6/7)	50 (1/2)	NS	82 (9/11)
NPV (%)	83 (5/6)	83 (5/6)	NS	70 (42/60)
Accuracy (%)	85 (11/13)	46 (6/13)	.048	72 (51/71)

**Note:**—PPV indicates positive predictive value, NPV, negative predictive value; NS, not statistically significant.

<sup>a</sup> Those cases with SWI sequences but read without the SWI sequences.

<sup>b</sup> Significance =  $P < .05$ .

<sup>c</sup> All cases read without SWI sequences.

**Table 3: Decision matrix data for the detection of calcification in ODs for MRnoSWI<sup>a</sup> versus CT (criterion standard)**

	CT+	CT-
MRnoSWI reading+	9	2
MRnoSWI reading-	18	42

**Note:**—+ indicates test was positive for calcification; -, test was negative for calcification.

<sup>a</sup>  $n = 71$ , unpaired.

in the phase relative to surrounding tissues due to susceptibility differences. The oxygen in diamagnetic oxyhemoglobin shields the iron so that the susceptibility effects are only seen in venous blood. This provides a natural separation of venous (deoxyhemoglobin) and arterial (oxyhemoglobin) blood and allows venographic images without any arterial contamination.<sup>9</sup> The sensitivity of SWI to iron is also used in the detection and demonstration of the extent of traumatic brain injury, stroke, vascular malformations and venous disease, deep vein thrombosis and blood settling, neurodegenerative disorders (multiple sclerosis, Alzheimer disease), and brain tumors.<sup>2</sup>

In the process of creating an SWI, the first 2 components provided are the original magnitude image and the raw phase image. The raw phase image is then HP filtered to remove unwanted artifacts. The magnitude image is then combined with the HP-filtered phase image to create an enhanced contrast magnitude image referred to as the SWI or the SW-filtered-phase image. For better visualization of vessel connectivity and microbleed locations, mIPs are created, usually over  $\geq 4$  adjacent SW images to create an effective 8- to 10-mm-thick section. In this way with SWI, we can generate a total of 5 sets of images: 1) the original magnitude image, 2) the raw phase image, 3) the HP-filtered phase image, 4) the SW-filtered phase image, and 5) the mIPs over the SW-filtered phase images.

SWI is predicted to detect calcium better than the traditional pulse sequences. We sought to assess the value of SWI not in its traditional role of looking for hemorrhage or prominent veins but to identify calcification and distinguish it from hemorrhage. Our study has demonstrated that intratumoral calcification cannot be reliably identified by conventional fast spin-echo MR imaging. The diverse signal intensities of calcium on conventional MR imaging make calcium very difficult to identify reliably.<sup>7,8</sup> However SWI can help differentiate calcification from hemorrhage because calcification is diamagnetic, whereas most hemorrhagic byproducts are paramagnetic. Due to the fact that calcium and iron have opposite magnetic susceptibilities, their phase deflections are opposite as well.<sup>4,10</sup> Negative phase shift (diamagnetic susceptibility)

occurs for veins, iron, and hemorrhage, making them appear uniformly dark. Calcium undergoes a positive phase shift (paramagnetic susceptibility) and is displayed as a high-signal-intensity area on the phase image.<sup>11</sup>

If a brain tumor like OD has both calcification and hemorrhagic components, SWI is an excellent tool to identify and differentiate one from the other. In a phase image, a hyperintense signal intensity indicates calcification. Hemorrhage and veins will appear dark (negative phase). The veins in a way serve as a control indicating that the bright signal intensity (positive phase) inside the tumor is a diamagnetic substance (ie, calcification).<sup>12</sup> In a retrospective study of 13 patients having calcified ODs, Zhu et al<sup>10</sup> demonstrated that the detection rate of calcification by SWI was significantly higher than by T1WI and T2WI ( $P < .05$ ). The independent sensitivity of SWI for intratumoral calcification detection in that study was 98.2% as opposed to 55.3% by T1WI and 73.2% by T2WI. Our study has confirmed the significantly superior sensitivity to intratumoral calcification of SWI (Fig 1). However, in the absence of calcification, no significant benefit to SWI was shown over traditional MR imaging pulse sequences.

ODs constitute 5%–20% of all glial tumors. It is predominantly a tumor of adulthood with a peak incidence between the fourth and sixth decade of life. No causative environmental or lifestyle factors have been identified. Loss of *1p/19q* has been identified as a characteristic genetic lesion. A clear association exists between codeletion of *1p* and *19q* and a classic histologic appearance (perinuclear halo, chicken wire vascular pattern).<sup>13,14</sup> Most ODs arise in the white matter of the cerebral hemispheres, predominantly in the frontal lobes. Most are well-differentiated WHO grade 2 diffusely infiltrating tumors and are composed predominantly of cells morphologically resembling oligodendroglia. Microscopic examination of tumor tissue is mandatory for the final diagnosis and, therefore, for initiating appropriate treatment. Low-grade tumors may be cured with surgery alone. Anaplastic/high-grade (WHO grade 3) features include high cell attenuation, mitosis, nuclear atypia, microvascular proliferation, and necrosis. These tumors are treated aggressively with resection, chemotherapy, and radiation therapy.<sup>15</sup> In anaplastic grade 3 ODs, codeletion of *1p* and *19q* is a marker for a better response to chemotherapy, durable tumor control after radiation therapy, and long overall survival. In low-grade ODs, it predicts a very favorable natural history.<sup>14,16,17</sup> The pathologic grade of the tumor is the single most important prognostic factor significantly affecting overall survival.<sup>18</sup>

Why should one care that SWI provides the advantage of identifying intratumoral calcification? Intratumoral calcifica-

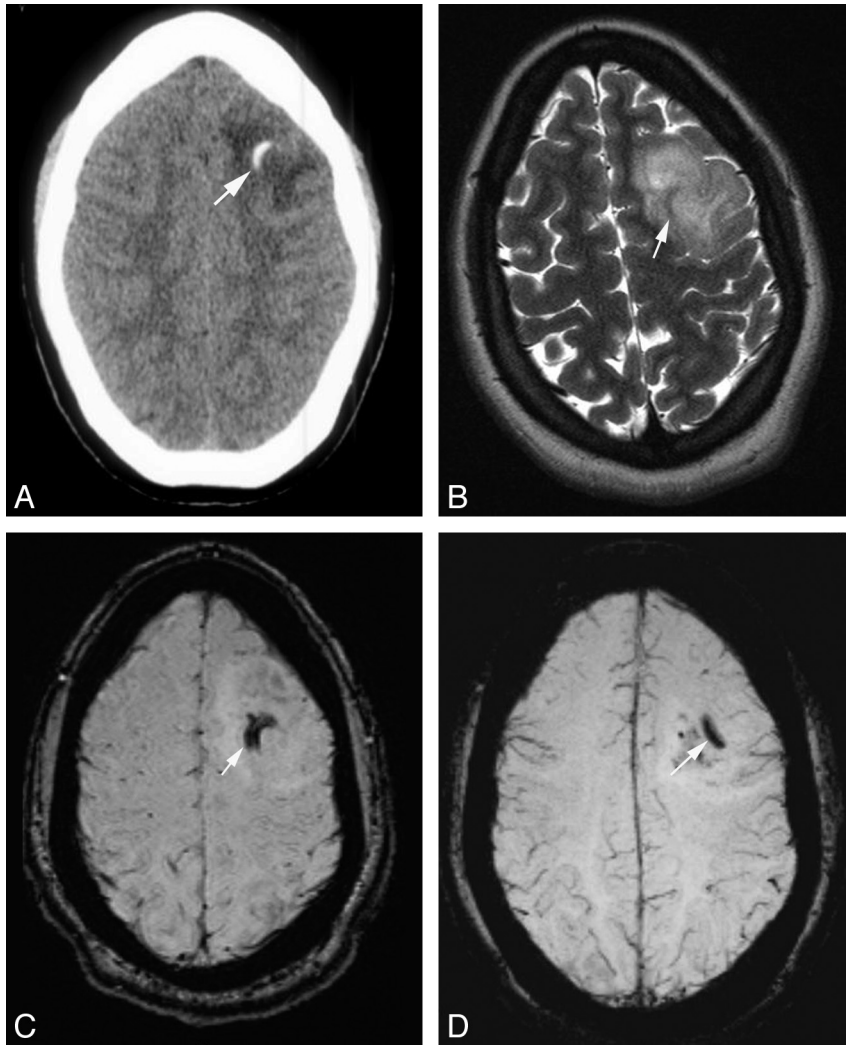


**Fig 1.** Imaging findings of a 23-year-old woman with a histopathologic diagnosis of OD. *A*, CT shows a  $2.3 \times 3.3$  cm ill-defined relatively hypoattenuated mass in the left frontal lobe with curvilinear calcification (arrow). There is no hemorrhage. *B*, T2WI image shows an intermediate-to-hyperintense lesion. The area of calcification by CT is seen on the MR imaging study, but it is hypointense and, therefore, is not suggestive of calcification (arrow). *C*, SWI image shows curvilinear calcification (hypointense area). *D*, SWI mIP image shows calcification.

tion is a very important factor in the differential diagnosis of brain tumors.<sup>12</sup> Although the likelihood of an OD is high for a calcified supratentorial intraparenchymal tumor,<sup>19,20</sup> the differential diagnosis of a calcified intra-axial intracranial mass includes other tumors as well, including ependymomas and low-grade astrocytomas. Therefore, the final diagnosis, while limited, is always made on histopathology. Dense coarse calcifications are seen in 34%–80% of ODs,<sup>6</sup> making ODs the intra-axial tumor with the highest frequency of calcification among brain tumors.<sup>15</sup> Our value of 38% (27/71 ODs) is at the lower range of the spectrum previously reported, possibly because of a sampling bias of recurrent tumors that are sent to our institution. Not all patients with OD had CT scans performed to verify the calcification.

Why should one care if an OD does or does not have intratumoral calcification? Patients with calcified ODs had significantly longer survival rates than the corresponding patients without calcification in the study of Martin and Lemmen.<sup>19</sup> Similarly in Shimizu et al,<sup>21</sup> the calcified ODs had a favorable prognosis; the 5-year survival rate was 67% with calcification compared with 33% in patients without any. Tumors with

*1p/19q* loss have a significant association with intratumoral calcification<sup>17</sup> and paramagnetic susceptibility effect (caused by tumor-associated hemorrhage).<sup>22</sup> One might speculate that calcification is a biologic event downstream of *1p* and *19q* loss and, therefore, a marker for the *1p/19q* codeletion in ODs, but perhaps calcification is not the direct result of this genetic predisposition. There is a strong possibility that calcification might be the feature of the slow growth and indolent course of most ODs with the *1p/19q* codeletion. Second, in addition to often being calcified, ODs with *1p* and *19q* loss contain paramagnetic (hemorrhagic) elements.<sup>17,22</sup>

Although patients with calcified gliomas survive longer, thereby giving intratumoral calcification and its detection a perceptible prognostic importance, this length of survival may be more closely related to the histologic grade of malignancy of the tumor rather than to calcification alone. Because it is not possible to tell the grade of the malignancy from the radiologic appearances of the calcium deposits, it follows that glioma calcification by itself is of significantly less value in prognosis than in grade. Also even though calcification is more common in slow-growing gliomas, the presence of calcification does not

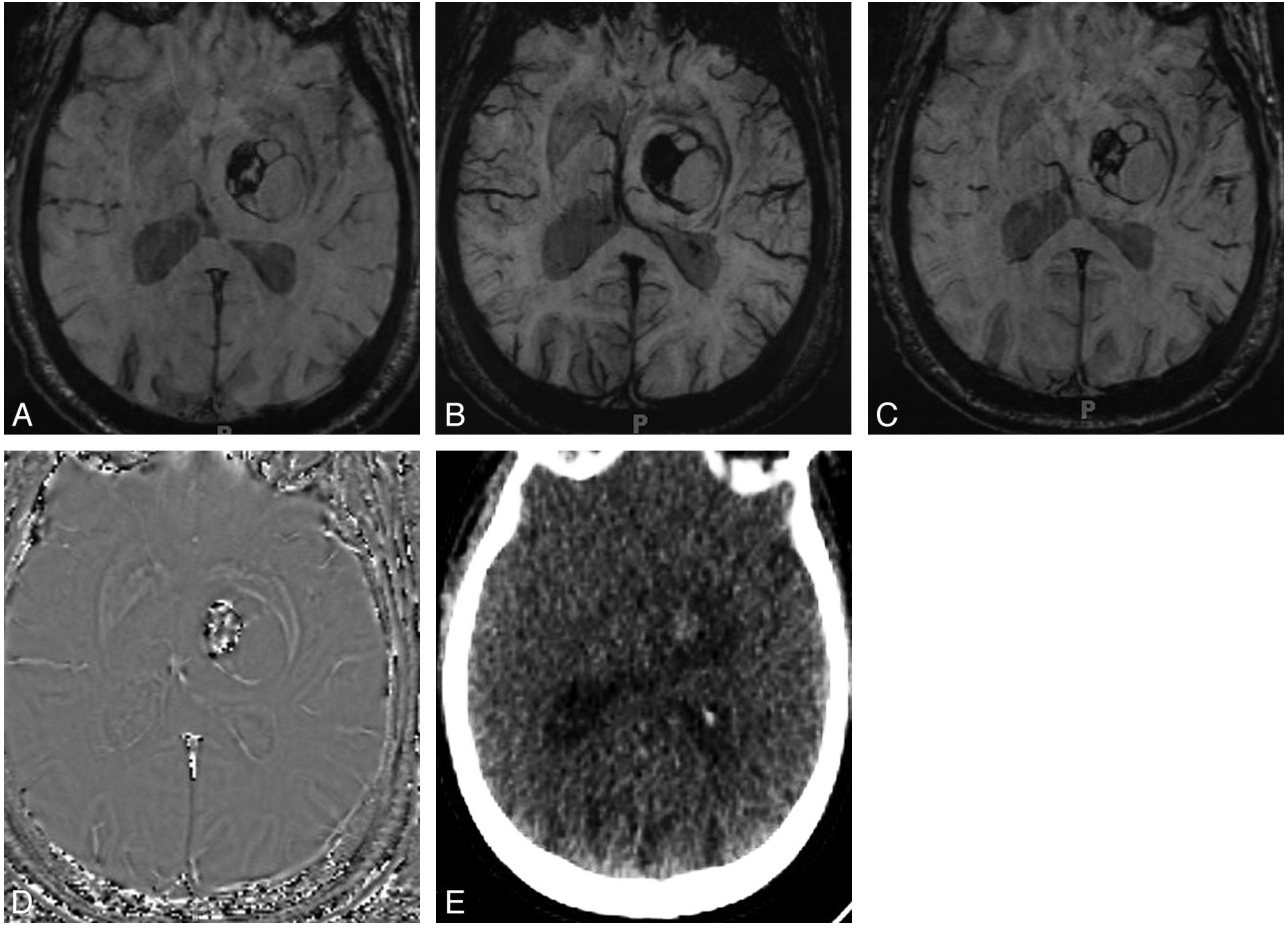


**Fig 2.** Value of phase imaging in identifying calcification in OD. Magnitude (A), mIP (B), and SWI (C) images do not help distinguish iron-containing hemorrhage from calcification in this tumor. D, Phase image shows high signal intensity centrally identifying calcification. E, CT image shows faint hyperattenuation, which had persisted for months and represented calcified tumor.

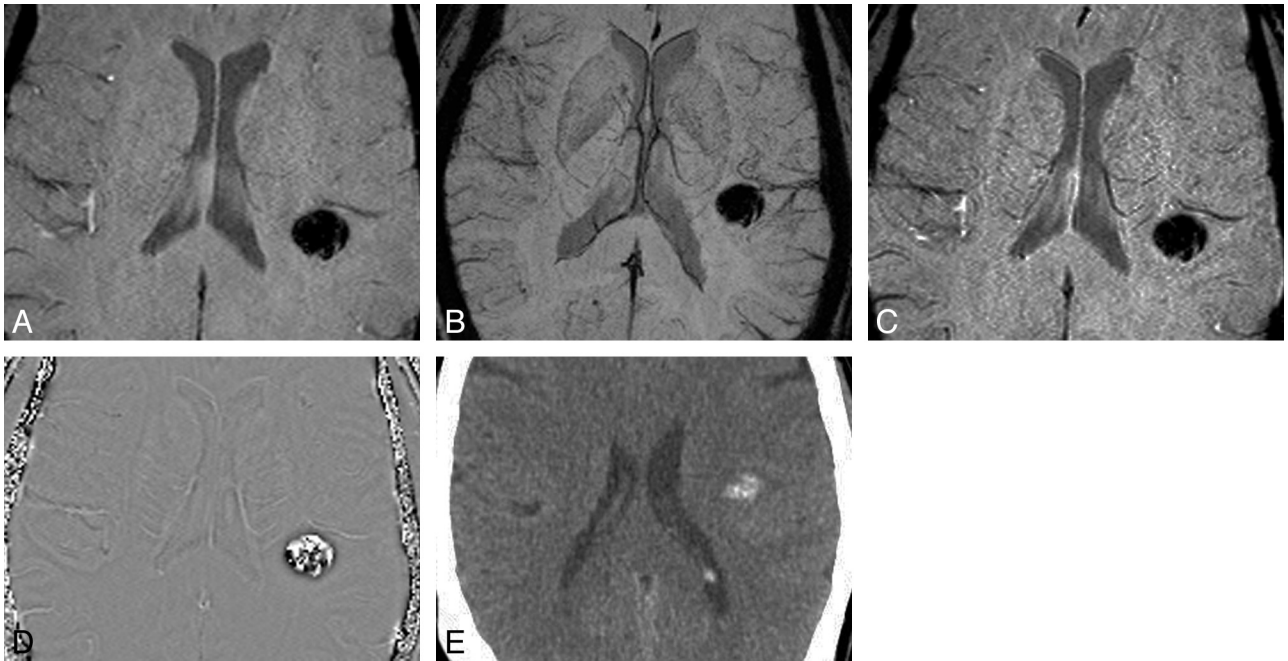


**Fig 3.** Calcification on SWI series. Again, the magnitude (A), mIP (B), and SWI (C) images could represent hemorrhage or calcification. D and E, However, the phase image (D) shows hyperintensity of calcification, confirmed on the CT scan (E).

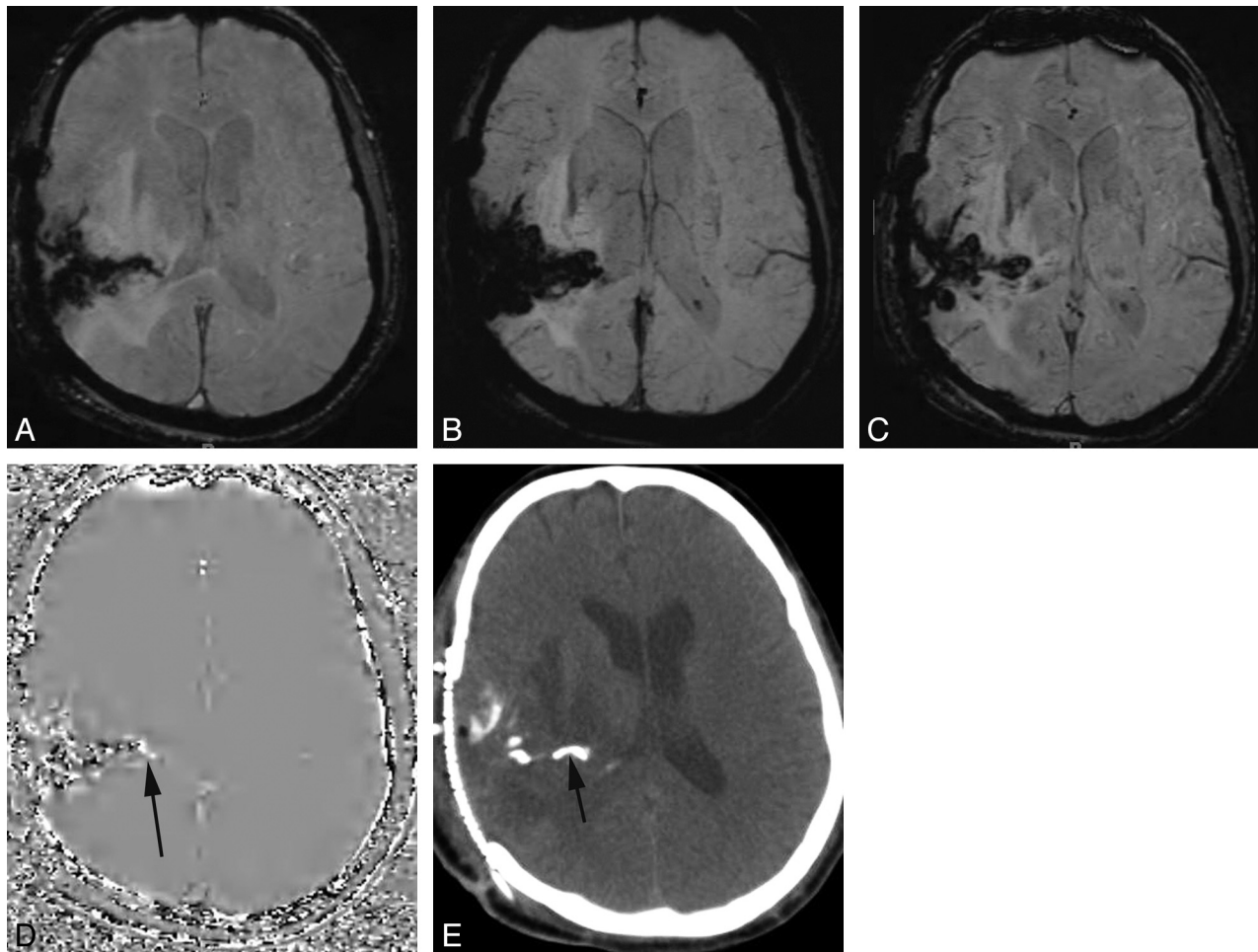


**Fig 4.** Postoperative OD with hemorrhage and calcification. Magnitude (A), mIP (B), and SWI (C) images fail to distinguish hemorrhage in the operative bed from calcification. D and E, Phase images show mixed signal intensity, but an area of high signal intensity more medially (arrow) was read as representing calcification. CT confirmed a calcified component (arrow).

exclude a rapidly growing tumor. Moreover, the extent of the calcification bears no relation to the actual size of the tumor.<sup>23</sup> In a nutshell, calcification in a glioma is an indication of its relatively low grade rather than absolute benignity.<sup>24</sup>

The limitations of this work include our small sample size because ODs are rare tumors and SW studies of these tumors have only been used at our institution in the past 2 years. The scanning intervals between the MR imaging and CT examinations and/or intervening surgery might have obscured some results. It is possible that SWI may have detected calcification before CT. Is the CT still the best criterion standard for this study? Because we used 3 different manufacturers and both 1.5T and 3T scanners, the study population is inhomogeneous. Our observational study design led to variable protocols used and the unavailability of phase images in all subjects. Thus, this retrospective study may be considered as a pilot for more extensive and prospective studies to come.

### Conclusions

Using CT scanning as the criterion standard for intratumoral OD calcification, we found that SWI can detect calcification better than traditional pulse sequences. SWI is unlikely to replace CT for the detection of intratumoral calcification, but because MR imaging has become the primary means for detecting tumors in patients with seizures, headaches, and neu-

rologic deficits, SWI sequences may be helpful for suggesting the diagnosis of OD. This is increasingly true as radiation safety concerns shift the imaging work-up from CT to MR imaging. The presence of intratumoral calcification has a complex relationship with tumor grade and prognosis.

### References

1. Haacke EM, Mittal S, Wu Z, et al. **Susceptibility-weighted imaging: technical aspects and clinical applications, part 1.** *AJNR Am J Neuroradiol* 2009;30:19–30
2. Haacke EM, Cheng NY, House MJ, et al. **Imaging iron stores in the brain using magnetic resonance imaging.** *Magn Reson Imaging* 2005;23:1–25
3. Mittal S, Wu Z, Neelavalli J, et al. **Susceptibility-weighted imaging: technical aspects and clinical applications, part 2.** *AJNR Am J Neuroradiol* 2009;30:232–52
4. Gupta RK, Rao SB, Jain R, et al. **Differentiation of calcification from chronic hemorrhage with corrected gradient echo phase imaging.** *J Comput Assist Tomogr* 2001;25:698–704
5. Margain D, Peretti-Viton P, Perez-Castillo AM, et al. **Oligodendrogliomas.** *J Neuroradiol* 1991;18:153–60
6. Leonardi MA, Lumenta CB. **Oligodendrogliomas in the CT/MR-era.** *Acta Neurochir* 2001;143:1195–203
7. Oot RF, New PF, Pile-Spellman J, et al. **The detection of intracranial calcifications by MR.** *AJNR Am J Neuroradiol* 1986;7:801–09
8. Avrahami E, Cohn DF, Feibel M, et al. **MRI demonstration and CT correlation of the brain in patients with idiopathic intracerebral calcification.** *J Neurol* 1994;241:381–84
9. Barnes SR, Haacke EM. **Susceptibility-weighted imaging: clinical angiographic applications.** *Magn Reson Imaging Clin N Am* 2009;17:47–61
10. Zhu WZ, Qi JP, Zhan CJ, et al. **Magnetic resonance susceptibility weighted**

- imaging in detecting intracranial calcification and hemorrhage.** *Chin Med J (Engl)* 2008;121:2021–25
11. Yamada N, Imakita S, Sakuma T, et al. **Intracranial calcification on gradient-echo phase image: depiction of diamagnetic susceptibility.** *Radiology* 1996;198:171–78
  12. Wu Z, Mittal S, Kish K, et al. **Identification of calcification with MRI using susceptibility-weighted imaging: a case study.** *J Magn Reson Imaging* 2009;29:177–82
  13. McDonald JM, See SJ, Tremont IW, et al. **The prognostic impact of histology and 1p/19q status in anaplastic oligodendroglial tumors.** *Cancer* 2005;104:1468–77
  14. Aldape K, Burger PC, Perry A. **Clinicopathological aspects of 1p/19q loss and the diagnosis of oligodendrogliomas.** *Arch Pathol Lab Med* 2007;131:242–51
  15. Van den Bent MJ, Reni M, Gatta G, et al. **Oligodendroglioma.** *Crit Rev Oncol Hematol* 2008;66:262–72
  16. Cairncross JG, Ueki K, Zlatescu MC, et al. **Specific genetic predictors of chemotherapeutic response and survival in patients with anaplastic oligodendrogliomas.** *J Natl Cancer Inst* 1998;90:1473–79
  17. Van den Bent MJ, Looijenga LH, Langenberg K, et al. **Chromosomal anomalies in oligodendroglial tumors are correlated with clinical features.** *Cancer* 2003;97:1276–84
  18. Edward S, Bernd S, Judith R, et al. **Oligodendroglioma: the Mayo Clinic experience.** *J Neurosurg* 1992;76:428–34
  19. Martin F, Lemmen LJ. **Calcification in intracranial neoplasm.** *Am J Pathol* 1952;28:1107–31
  20. Lee YY, Van Tassel P. **Intracranial oligodendrogliomas: imaging findings in 35 untreated cases.** *AJR Am J Roentgenol* 1989;152:361–69
  21. Shimizu KT, Tran LM, Mark RJ, et al. **Management of oligodendrogliomas.** *Radiology* 1993;186:569–72
  22. Megyesi JF, Kachur E, Lee DH, et al. **Imaging correlates of molecular signatures in oligodendrogliomas.** *Clin Cancer Res* 2004;10:4303–06
  23. Kalan C, Burrows EH. **Calcification in intracranial gliomata.** *Br J Radiol* 1962;35:589–602
  24. Courville CB, Adelstein LJ. **Intracranial calcification, with particular reference to that occurring in the gliomas.** *Arch Surg* 1930;21:801–28